Adsorption (2015) 21:25–35
DOI 10.1007/s10450-014-9647-3

Easily tunable parameterization of a force field for gas adsorption on FAU zeolites

Victor A. M. Gomes · Juliana A. Coelho · Hugo R. Peixoto · Sebastião M. P. Lucena

Received: 4 July 2014 / Revised: 20 December 2014 / Accepted: 23 December 2014 / Published online: 30 December 2014

Abstract Considering the great economic and environmental interests in the capture and separation of CO_2 and the wide availability of faujasites zeolites (FAU), we propose a set of parameters based on classical force fields that has good transferability among Na-FAU sieves and CO_2. In addition to CO_2, the parameterization strategy was tested for H_2S, O_2, N_2 and CH_4 gases. For these gases, the force field adequately predicts the adsorption isotherms at low pressure. The force field was also tested for N_2 in the FAU framework with different monovalent and divalent cations, resulting in quantitative agreement for monovalent cations and qualitative agreement for divalent cations. The good tradeoff between the reliability and ease of implementation will enable rapid evaluation of the adsorption properties of gaseous mixtures of industrial relevance. The reasoning of the re-parameterization strategy is also discussed in detail.

Keywords Molecular simulation · Adsorption · Carbon dioxide · Light gases and faujasite

1 Introduction

In recent years, there has been great demand to facilitate the use of adsorption processes for CO_2 capture (Su and Lu 2012; Bae et al. 2013; First et al. 2014) and the separation of toxic gases (Kumar et al. 2011; Tagliabue et al. 2012; Sun et al. 2014). On one hand, carbon dioxide, coming from several sources, is associated with methane (natural gas, shale gas, biogas), nitrogen (gas burning) or toxic gases, making it difficult to select materials and to design adsorption industrial units (PSA, TSA). On the other hand, zeolites based in sodalite units dominate the molecular sieve market. The LTA-type is the most frequently used zeolite, and the FAU-type zeolite is the second most used zeolite (Cejka et al. 2007).

Experimental isotherms for FAU crystals in low-pressure conditions were performed with CO_2 (Walton et al. 2006; Hyun and Danner 1982; Cavenati et al. 2004; Kim et al. 1994), N_2 (Jayaraman et al. 2002; Cavenati et al. 2004; Llewellyn et al. 2005; Kim et al. 1994), CH_4 (Cavenati et al. 2004; Pillai et al. 2010; Silva et al. 2012), O_2 (Jayaraman et al. 2002) and H_2S (Cruz et al. 2005). Despite the great interest of the scientific community on the subject, multicomponent experimental isotherms at low pressures in pure crystals remain scarce (Kim et al. 1994). This scarcity is due to the fact that the study of mixtures by experimental methods is costly and time-consuming.

Assisted by increased computer power, molecular simulation codes have been applied to support the screening phase, enabling the selection of suitable materials before proceeding to experimental work (First et al. 2014; Wilmer et al. 2012). Despite the demands for the use of zeolites in CO_2 capture and other applications, force fields optimized for FAU or LTA sieves for different gases are still rare, especially in the low pressure region, which is important for the gaseous mixtures cited. One reason for the lack of force fields is that modeling sodalite-based zeolites is a significant challenge because the frameworks are produced in different Si/Al ratios and may present different extra-

Electronic supplementary material The online version of this article (doi:10.1007/s10450-014-9647-3) contains supplementary material, which is available to authorized users.

V. A. M. Gomes · J. A. Coelho · H. R. Peixoto · S. M. P. Lucena (✉)
Grupo de Pesquisa em Separações por Adsorção – GPSA, Dept. Engenharia Química, Universidade Federal do Ceará, Campus do Pici, Bl. 709, Fortaleza, CE 60455-760, Brazil
e-mail: smlucena@uol.com.br

framework cationic species. Most force fields are devoted only to CO_2 (Maurin et al. 2005a; García-Sánchez et al. 2009; Fang et al. 2013). When more than one gas is studied, the force field is optimized for only a sodalite-based zeolite (Akten et al. 2003; Jaramillo and Chandross 2004) or single component isotherms for CO_2 were not computed (Kiselev and Du 1981; Watanabe and Stapleton 1995; Calero et al. 2004) (Table 1).

Aiming to overcome this deficiency in the literature, we followed a few simple guidelines and found a force field parameter set that can be easily tunable to different molecules on FAU frameworks. These guidelines were:

(1) Wise choice of the existing force fields approach, exploiting a large database that has been constructed over more than three decades (since Bezus et al. 1978).
(2) Optimization of parameters guided by the experimentally predicted crossover pressure between CO_2 isotherms on NaX and NaY at low pressure (<100 kPa). The crossover pressure is similar to an inflection point, which is caused by a subtle interplay between the number and positioning of cations. The low loading regime imposed by the sieve-gas interaction starts to change to the higher loading regime, as determined by the gas–gas molecules interaction. The use of inflection points avoids those parameters with unphysical meaning (Dubbeldam et al. 2004).
(3) Only one degree of freedom is allowed for tuning the force field. The parameter defined was the Lennard-Jones (LJ) energy parameter (ε) of the tetrahedral species, which is limited to a minimum value of zero and a maximum value that is equal to that proposed by the UFF force field (Rappé et al. 1992). Often in zeolite/adsorbate systems, limitations in the models of molecules, defects in the framework and forces of interaction (e.g., induction) are not embedded in the model. Those effects were taken into account in an implicit way by fitting the atomic charges of the framework atoms or the LJ parameters (Calero et al. 2004). The degree of freedom in the tetrahedral species parameters can therefore be interpreted as an implicit fitting of these uncertainties that is associated with the nature of the system investigated. As the only exception to this guideline, we decreased the site III charge to enable NaX experimental isotherm fitting for H_2S. Note that this is the first force field to reproduce experimental H_2S equilibrium properties in the FAU framework.

Our parameter set represents a reasonable tradeoff between reliability and ease of implementation. This parameter set will be useful to gain insight and rapid screening of the FAU frameworks, thereby enabling implementation in more generic Monte Carlo codes lacking specialized techniques (e.g., Materials Studio by Accelrys, Materials Design, SPPARKS, MCCCS Towhee) and facilitating the use of molecular simulation by experimentalists.

2 Modeling

2.1 Force fields and re-parametrization strategy

We assume that the gas/FAU system can be properly described using the LJ potential for repulsion-dispersion forces plus Coulombic contributions between point charges:

$$U(r_{ij}) = 4\varepsilon_{ij}\left[\left(\frac{\sigma_{ij}}{r_{ij}}\right)^{12} - \left(\frac{\sigma_{ij}}{r_{ij}}\right)^{6}\right] + \frac{q_i q_j}{r_{ij}}$$

where ε_{ij} is the well depth, σ_{ij} is the equilibrium diameter, and r_{ij} is the distance between interacting atoms i and j. In the second term, q_i and q_j are point charges separated by the distance r_{ij}. The cross LJ terms were obtained using the usual arithmetic and geometric combination rules.

Table 1 Proposed force fields for adsorption of gases on sodalite-based zeolites

Reference	Gases	Sodalite-based zeolite
Kiselev and Du 1981 (*)	Ar, Kr, Xe, O_2, N_2, CO, CO_2, NH_3	NaX, NaY
Watanabe and Stapleton 1995	N_2, O_2, Ar	5A, CaA, NaA, CaX, NaX, NaY
Akten et al. 2003	CO_2, N_2, H_2	NaA
Jaramillo and Chandross 2004	CO_2, NH_3	NaA
Calero et al. 2004	Alkanes (C1 to C5)	NaX, NaY
Maurin et al. 2005a	CO_2	NaX, NaY, USY
Maurin et al. 2005b	N_2	NaX
García-Sánchez et al. 2009	CO_2	NaX, NaY
Fang et al. 2013	CO_2	NaA, NaX, NaY

(*) Henry's coefficient and internal energy

Table 2 Main force field framework-related issues

Reference	LJ Si and Al atoms	Charge Si and Al atoms	Na Charge	Na move	Overall charge neutrality
Kiselev and Du 1981	No	No	Partially ionized	No	Oxygen
Watanabe and Stapleton 1995	Yes	Yes	Partially ionized	No	Si and Al
Maurin et al. 2005a	No	Yes	Partially ionized	No	–
García-Sánchez et al. 2009	No	Yes	Partially ionized	Yes	–
Fang et al. 2013	Yes	Yes	Partially ionized	Yes	Oxygen
This study	Yes	Yes	Partially ionized	No	Oxygen

Some basic characteristics of the force field related to the framework must be defined a priori: the LJ parameters and charges to be assigned to Si and Al atoms; which atom species will provide overall charge neutrality; the Na charge (partially ionized or not) and Na mobility. The first proposal for FAU parameters, from the pioneering studies of Kiselev (Kiselev and Du 1981), set the charges and the LJ potential parameters on the Si and Al atoms as zero. The oxygen atom was used for overall neutrality, and all of the Na atoms were fixed and partially ionized in site III. Despite this approximation, good agreement between the computed and measured heats of adsorption for Ar, Kr, Xe, O_2, N_2, CO, CO_2 and NH_3 on NaX and NaY was found. Watanabe and Stapleton (1995) optimized a force field that reproduces the experimental isotherms of N_2, O_2 and Ar in A, X and Y zeolites, incorporating the parameters of the interactions between the Si and Al atoms that were neglected by Kiselev. The atoms of Si and Al were set for overall neutrality. Maurin et al. (2005a) developed a force field that reproduces the differential enthalpies and adsorption isotherms at high pressures for CO_2 in NaY, NaX and USY (dealuminated) zeolites. In this parameterization, similar to that performed by Kiselev, the contribution of Si and Al atoms in the LJ interaction potentials was neglected, but the electrostatic contributions were considered. García-Sánchez et al. (2009) developed a force field dedicated to reproducing the CO_2 adsorption on different zeolites (MFI, MOR, 4A and FAU-Y). No LJ parameters are assigned to Si and Al, and the Na cations were unconstrained. Although the authors were particularly successful, the optimization simplex algorithm that was used gave rise to an entirely new set of LJ parameters and charges. Additionally, the extra LJ parameter ($Na–O_{zeolite}$) that was introduced to allow the Na motion during the simulation added complexity to the model, which reduced the transferability between different gases and cation species. Akten et al. (2003), for example, used a similar approach for CO_2, N_2 and H_2 in the 4A zeolite, and several new interaction parameters had to be introduced between each gas and the zeolite oxygen to generate agreement between the experimental and simulated isotherms. Recently, Fang et al. (2013) proposed a force field for CO_2 on a 4A sieve based entirely on quantum methods. The LJ parameters and charges were assigned to Si and Al, oxygen was used to provide overall neutrality and Na cations were unconstrained. A summary of the force field characteristics discussed, highlighting our choices, is presented in Table 2. Despite the trend to add movement to the cations, in this study, we chose to keep them fixed. This decision is related to experimental evidence and also to the impact caused by the motion of cations in the simulated isotherms. Wong-Ng et al. (2013) experimentally found that of the 27 site II cations, only seven migrate to site II* when CO_2 was adsorbed at 100 kPa and room temperature in NaY. There is no experimental evidence that the atoms in sites I or II assume positions at site III. We simulated the impact of the configuration with seven atoms in site II* and observed that the adsorbed amount remain unchanged. Calero et al. (2004) confirmed the small impact that cations displacement causes in the adsorption isotherm of light gases. When adsorbing butane, the simulation results indicated that 16 cations of zeolite $Na_{58}Y$ migrate to position III. Even with this high displacement, the simulated isotherm, considering cation mobility, exhibited only a marginal improvement in the reproduction of the experimental isotherm.

2.2 Parameters of the frameworks

The lattices for all of the faujasite frameworks were constructed based on the structural parameters reported by Fitch et al. (1986), which has been used in others simulation studies (Maurin et al. 2005a; Garcia-Sanchez et al. 2009; Watanabe and Stapleton, 1995). The Fitch structure crystallizes in the space group Fd3 m (cell length = 24.85 Å). Silicon atoms were randomly replaced by aluminum atoms, obeying the Lowenstein rule (Lowenstein, 1954), where Al–O–Al bonds are not allowed. All of the sodalites were blocked to prevent gas molecules from being randomly generated inside the sodalite cavities during Monte Carlo moves.

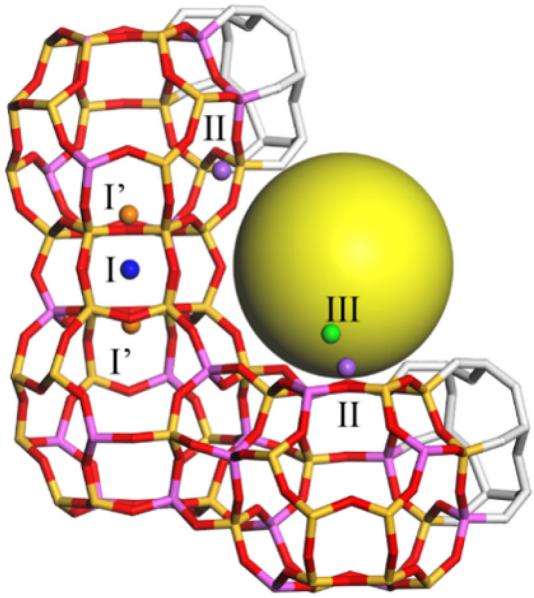

Fig. 1 Faujasite cation positioning. SI-*blue*, SI'-*orange*, SII-*purple* and SIII-*green*. *Yellow sphere*—pore volume of the supercage

Faujasite have cations distributed symmetrically in sites I, I', II and III (Fig. 1). Site I is positioned in the center of the hexagonal prism, while I' is at the interface between the sodalite and the hexagonal prism. These sites are not exposed and do not directly interact with the adsorbates. The site II cations are in the supercage, coordinating with three oxygens from the 6-ring window of the sodalite cage. The cations in site III are above the 4-ring window, close to the side of a 12-ring window.

For NaX, the extra framework sodium cation distribution was based on Zhu and Seff (1999) and Di Lella et al. (2006) for the Si/Al ratios of 1.23 ($Na_{86}Al_{86}Si_{106}O_{384}$) and 1.49 ($Na_{77}Al_{77}Si_{115}O_{384}$), respectively. These Si/Al ratios of 1.23 and 1.49 correspond to a framework with 86 cations, (32 in site II, 32 the site I', 22 in site III) and 77 cations (32 in site II, 32 in site I' and 13 site III), respectively.

The NaY cation distribution was based on the 2.31 Al/Si ratio ($Na_{58}Al_{58}Si_{134}O_{384}$) reported by Fitch et al. (1986) with 58 cations (29 in site II and 29 in site I'). All of the sodium atoms are randomly added until the distribution for each structure is achieved.

We did not differentiate the Al atom distribution in the framework. Quantum studies calculated at various levels of theory (Thang et al. 2014; Plant et al. 2006) found little impact of the Al distribution in adsorption. Thang found a difference of only 5 % between the site's potential with one and two atoms of Al and found that the site II population with one aluminum atom was estimated at only 18 % (FAU with Si/Al ratio = 2.5). Plant performed similar calculations for the adsorption of ethanol and found differences of the potential of the same order of magnitude between one and two Al atoms in the window 6R. Only configurations with three Al atoms increased the potential by 17 % due to the formation of hydrogen bonds between the methanol and the cations, which does not occur with CO_2.

2.2.1 Charges

The point charges of Si, Al and Na_{II} in the zeolites were assigned using the charge equilibration method (Rappé and Goddard 1991). The charges are close to the others studies that apply charge equilibration (Takahashi et al. 1996; Kitagawa et al. 1996). Additionally, partially ionized cations were used in most FAU and LTA simulation studies (Table 2). Our charges were optimized to provide the same USY charge equilibration calculation values in the absence of aluminum and sodium. The oxygen charge was chosen to retain the electroneutrality of the lattice. Our charge set (except for Na) was also similar to that of Uytterhoeven et al. (1992), which was obtained for NaY and USY using the electronegativity equalization method (EEM), an approach based in density functional theory. The charge of the Na in position III was established using the study by Kiselev and Du (1981) and optimized using experimental CO_2 isotherms from NaX. Kiselev considered the Na charge in site III to be lower than that in site II when the adsorption of CO_2 and other gases was simulated in NaX. Recent quantum studies supported the use of a distinct charge for the cation in site III. Sung et al. (2012), from quantum chemical calculations, found that the charge of alkali cations (Li, Na and K) in site II was decreased by 10–22 % (by transferring electron) in the presence of CO_2 and H_2S gases. Unfortunately, the calculations for the cations in site III were not performed; such calculations are beyond the scope of our study. However, it is implicit that, as the site III cations interact strongly with the adsorbate than site II cations, there must be a difference in charge between these two sites. Our proposal was a 20 % decrease (for CO_2, O_2, N_2 and CH_4) and 45 % decrease (for H_2S). H_2S is a special case because there is experimental evidence that the site III cations (not occurring with the site II cations) cause the dissociation of H_2S (Karger and Raskó 1978). For other gases, there is no experimental evidence of dissociation; site III (and to a lesser extent the site II) only causes a partial ionization of the gas without any dissociation (Sung et al. 2009).

2.2.2 LJ parameters

Having obtained the charges via the charge equilibration method, we chose the LJ parameters from the UFF force field (Rappé et al. 1992) because the partial charges in this

force field were also obtained using the charge equilibration method. We apply the original LJ UFF parameters to all of the framework atoms. By simulating the CO_2 isotherms in NaY, we observed that the adsorbed values were overestimated by more than 40 % relative to the experimental values. Because Kiselev and Du (1981), Maurin et al. (2005a) and Garcıa-Sanchez et al. (2009) set the LJ parameter for Si and Al to zero, the energy parameter (ε) for Si and Al suggested by the UFF force field were reduced. The experimental and simulated isotherms matched when ε for Si and Al correspond to 22.5 % of the full UFF value. In this stage of re-parameterization, only experimental data from CO_2 in NaY were used as a calibration point. We also adopted an epsilon value for the oxygen atom that is 15 % larger than the original UFF parameter, further helping to improve the agreement between the experimental and simulated isotherms. All of the LJ parameters and charges are presented in Table 3.

2.3 Gases molecules parameters

The CO_2 model was taken from Harris and Yung (1995). This model has three charged sites, where $q = +0.656$ is the charge of the carbon and $-q/2$ is the charge in the oxygen sites. The center of the oxygen atoms was separated by a length of 2.232 Å. The model accurately reproduces the vapor–liquid equilibrium data of CO_2 used in the Monte Carlo simulations (GCMC) to calculate the CO_2 adsorption on activated carbon and charged adsorbents, such as zeolites and MOFs (Garcia-Sanchez et al. 2009; Liu and Yang 2006; Liu et al. 2013).

For H_2S, we choose the Kristof and Liszi model (Kristof and Liszi, 1997). The model has the following parameters: S–H bond length of 1.340 Å, H–S–H angle of 92° and four charged sites ($q_H = +0.25$, $q_S = +0.4$, $q_{4th} = -0.9$). The model predicts the properties of the liquid and solid states and the H_2S vapor–liquid equilibrium. The nitrogen model was developed by Kaneko et al. (1994) and reproduces the quadrupole moment of the molecule. The distance between the centers of nitrogen is 1.094 Å. The model has four charged sites ($q = 0.373$) positioned outside the centers of mass of nitrogen atoms. The model of the oxygen molecule has a distance between the atoms of 1.21 Å and three charged sites to better reproduce the quadrupole moment ($q_O = -0.112$, $q_{central} = +0.224$) (Watanabe and Stapleton 1995).

The methane model was taken from the study of Skarmoutsos et al. (2005), which provides excellent results in the vapor–liquid equilibrium prediction. All of the atoms present in the molecule are represented explicitly. The length of bond C–H is 1.094 Å. The model has charges assigned to the atoms of hydrogen and carbon ($q_H = +0.06$, $q_C = -0.24$). Table 4 presents the parameters for the all of the gas models used.

Table 4 Simulation parameters for the adsorbates (for charges see text)

Model	CO_2	H_2S	N_2	O_2	CH_4
Charged sites	3	4	4	3	4
ε_C (kcal/mol)	0.056	–	–	–	0.066
ε_O (kcal/mol)	0.16	–	–	0.108	–
ε_{H2S} (kcal/mol)	–	0.496	–	–	–
ε_N (kcal/mol)	–	–	0.075	–	–
ε_H (kcal/mol)	–	–	–	–	0.03
σ_C (Å)	2.757	–	–	–	3.5
σ_O(Å)	3.03	–	–	3.05	–
σ_{H2S} (Å)	–	3.73	–	–	–
σ_N (Å)	–	–	3.318	–	–
σ_H (Å)	–	–	–	–	2.59

2.4 Computational details

The Monte Carlo method (GCMC) is used to calculate the equilibrium properties and the adsorption isotherms. The algorithm computes four basic movements: translation,

Table 3 LJ and Coulombic original parameters set for FAU

	Si	Al	O	Na(I' e II)	Na(III)
σ (Å)	3.826[b]	4.008[b]	3.118[b]	2.657[b]	2.657[b]
ε (kcal/mol)	0.092[c]	0.116[c]	0.070[c]	0.030[b]	0.030[b]
q (e^-)	+1.208[a]	+1.200[a]	−0.751 $O_{NaX(*)}$ −0.719 $O_{NaY(**)}$ −0.604 O_{USY}	+0.768[a]	+0.61[c]

[a] charge equilibration

[b] UFF

[c] this work

(*) NaX Si/Al = 1.23, (**) NaY Si/Al = 2.31

rotation, creation and destruction. Equilibrium is achieved when the chemical potential of the gas inside the zeolite pores equals the chemical potential of the free gas outside of the pores; details of this method can be found elsewhere (Frenkel and Smit 2002). The algorithm allows the total adsorbed molecules (absolute isotherm) to be calculated; the excess value is obtained by subtracting the simulated value by the number of molecules related to the molar volume (constant P and T) that is calculated using the Peng–Robinson equation (Gusev et al. 1997; Davis and Seaton 1998; Lucena et al. 2010).

The simulations were performed on a Dell workstation (Intel Xeon Quad-Core), using the sorption module in the Materials Studio from Accelrys. The cut-off was 12.5 Å, with a lower boundary at 0.4 Å, similar to those used in FAU systems (Liu and Yang 2006; Kitagawa et al. 1996; Calero et al. 2004). We used 5×10^6 and 2.5×10^6 Monte Carlo steps during the equilibration and production phases, respectively.

3 Results and discussion

3.1 Adsorption isotherms

3.1.1 CO_2 molecule and the crossover pressure approach

It is important that the experimental data used in the parameter optimization comes from the same study to avoid variations of the experimental method and the origin of the samples. Experimental data for CO_2 adsorbed on NaX and NaY satisfying those conditions were found in the study performed by Walton et al. (2006). More experimental data for CO_2 can be found in Supplementary Information S1. The authors studied CO_2 adsorption at low pressures (up to 1 atm) for different monovalent cations in zeolite X (Si/Al = 1.23) and Y(Si/Al = 2.35). A crossover pressure is easily observed at 53 kPa (Fig. 2). NaX initially adsorbs more CO_2 than NaY; however, when the pressure exceeds 53 kPa, the amount adsorbed by NaX stabilizes to be overtaken by NaY. The crossover pressure can be explained by the interplay between the number of Na cations (that increase the adsorption heat) and the volume available for adsorption in the pores (that decrease as cation number increase). The X zeolite has 22 extra site III cations positioned inside the supercage. This cation population initially increases the amount adsorbed on zeolite X, but after 53 kPa, the uptake is limited by steric hindrance from the same cations. The isotherms crossover pressure is a signature for the FAU zeolites (types X and Y). The crossover pressure is caused by a subtle interplay between the number and the positioning of the cations. This behavior is a type of inflection point, in the sense that the

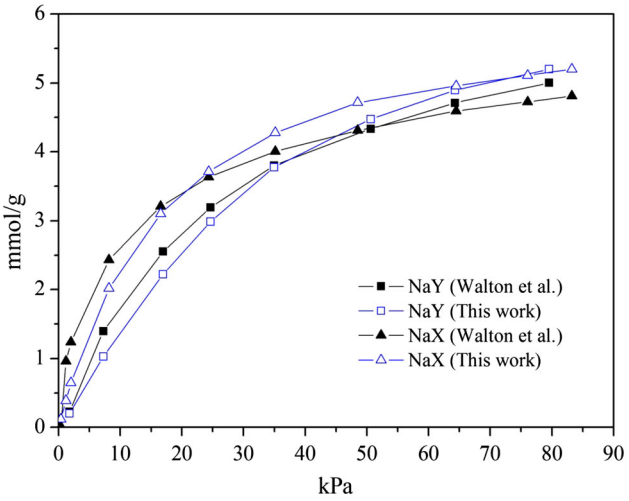

Fig. 2 CO_2 simulated (*open symbols*) and experimental (*closed symbols*) adsorption isotherms for NaX and NaY at 298 K

low loading regime imposed by the sieve interaction starts to change to the higher loading regime determined by the interaction of the adsorbed molecules. These are ideal isotherms to extract the most physically realistic parameters (Dubbeldam et al. 2004).

The crossover pressure signature was reproduced by the simulated data, as observed in Fig. 2. The simulated isotherms cross one another at 68 kPa. The agreement between each individual isotherm could be better; however, in this case, the crossover pressure is more important. To reproduce the crossover, the isotherms are of reduced accuracy. The simulated isotherms underestimate CO_2 adsorption at low pressure and overestimate it at high pressure. However, similar deviations are present in others force fields (Maurin et al. 2005a; Garcıa-Sanchez et al. 2009).

The first test of the new force field performance was to attempt to reproduce the experimental isotherm of CO_2 on USY zeolite. Compared to the experimental result reported by Maurin et al. (2005a) (Fig. 3), the simulated isotherm fit the experimental isotherm perfectly across the entire pressure range. This is a key result because, when adding cations to the structure, the experimental uncertainty for the positioning and quantity of the cations increases.

3.1.2 H_2S, N_2, O_2 and CH_4

We chose molecules that are normally found in mixtures with CO_2. The N_2 and O_2 gases may be present in combustion processes and CH_4 can be found in natural gas and biogas. H_2S represents the group of toxic gases that can occur in all cases cited.

We found H_2S experimental isotherms with the same characteristics as those used in the previous section for CO_2 (Cruz et al. 2005). The authors performed H_2S

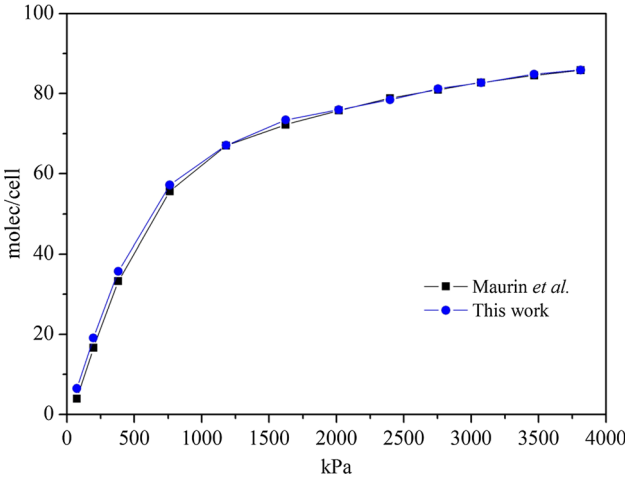

Fig. 3 CO_2 simulated (*blue symbols*) and experimental (*black symbols*) adsorption isotherms on USY at 298 K

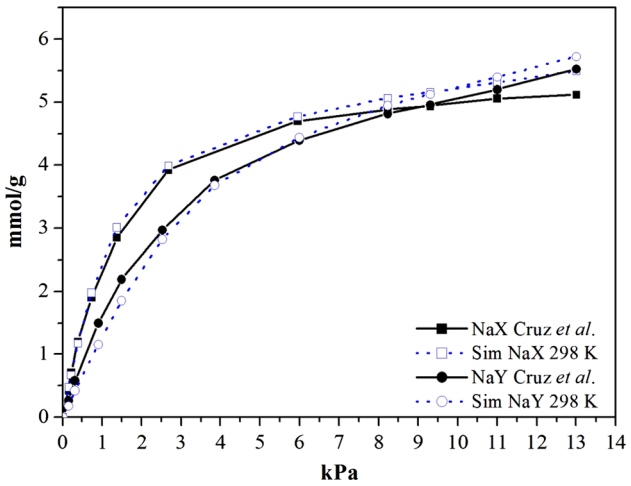

Fig. 4 Simulated (*open symbols*) and experimental (*closed symbols*) isotherms for H_2S on NaY and NaX at 298 K

adsorption measurements on zeolites NaX and NaY, and their data presented a crossover pressure at 9.2 kPa. The same CO_2 set of parameters was applied to the H_2S in the sieve NaY. As the simulated loading was less than the experimental loading, we utilize the degree of freedom defined previously: increase the value of the LJ parameters for the Si and Al atoms within the range from 0 to 100 % UFF.

The H2S isotherm on $Na_{58}Y$ was optimized to 35 % UFF (while CO_2 was optimized to 22.5 % UFF). Exceptionally, for $Na_{77}X$, besides the Si and Al LJ parameters set to 35 % UFF, we had to reduce the value of the Na charge in site III (+0.42). This decrease is due to dissociative interaction of H_2S in Na cations at site III, which our model does not take into account (Karge and Rasko 1978). Notably, we obtained almost the same pressure at which the experimental isotherms cross one another (9.2 kPa experimental and 9.8 kPa simulated—Fig. 4).

Experimental isotherms for N_2 and O_2 on $Na_{86}X$ were taken from the study of Jayaraman et al. (2002). For more experimental data, see Supp. Info. S1. As was performed for H_2S, the original parameters of the force field for CO_2 were applied to the two gases (Figs. 5, 6). While the O_2 simulated isotherms coincided perfectly, the simulated adsorbed amount of N_2 was less than the experimental amount. Re-parameterizing the values of epsilon for Si and Al, the simulated and experimental isotherms fit each other for 56 % UFF (Fig. 6). All errors were less than 3 %.

Finally, the experimental isotherm of CH_4 in the sieve $Na_{86}X$ was taken from the study Cavenati et al. (2004). See Supp. Inf. S1 for other experimental isotherms. Based on the original force field for CO_2, we obtained simulated adsorbed values below the experimental data. Fitting the epsilon parameters of Si and Al to 54 % UFF, allowed for

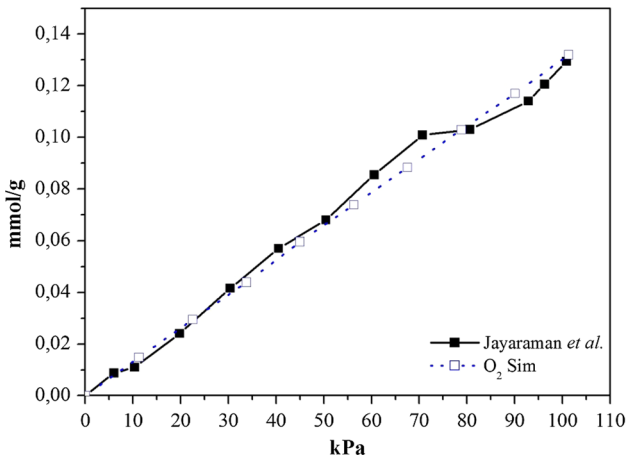

Fig. 5 Adsorption isotherms of O_2 on NaX at 300 K. (simulation—*blue*, experimental—*black*)

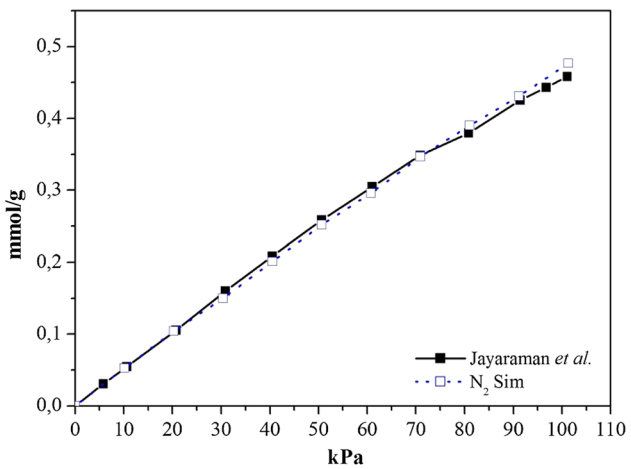

Fig. 6 Adsorption isotherms of N_2 on NaX at 300 K. (simulation—*blue*, experimental—*black*)

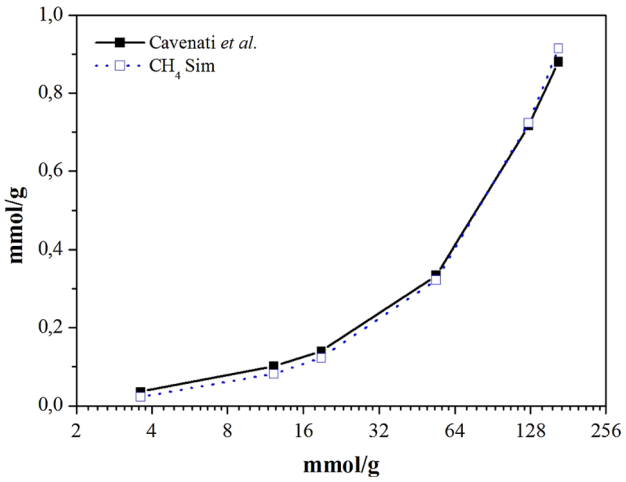

Fig. 7 Adsorption isotherms of CH_4 on NaX at 300 K. (simulation—*blue*, experimental—*black*)

the reproduction of the experimental isotherm (Fig. 7). The percentages in terms of the LJ parameter (ε_{Si} and ε_{Al}) for each gas species are presented in Table 5.

In addition to performing very well in predicting the adsorption of different gases, the physical nature of our force field should enable, for each gas studied, the prediction of the isotherms at other temperatures and for other mixtures as well as adsorption on FAU structures with different Si/Al ratios or with other cations. In the Supplementary Information, we present additional examples of the force field robustness (Supp. Inf. S3—mixture and S4—isotherms at other temperatures). In the next section, we will investigate how the force field performs for different cations.

3.2 Extra-framework cation species

One of the best agreements between the experiment and the simulation obtained for the adsorption properties involving a series of both monovalent and divalent cations were performed by Maurin et al. (2005b). They investigated the interaction between nitrogen and $M^{+}_{96}X$ ($M^{+} = Li^{+}$, Na^{+}, K^{+}) and $M^{2+}_{48}X$ ($M^{2+} = Ca^{2+}$, Mn^{2+}, Sr^{2+}, Ba^{2+}) frameworks. To test the transferability of our force field, we simulated the performance of nitrogen for the same series of X-FAU.

The framework positioning of the cations follows the same on that was used in the study of Maurin (Maurin et al. 2005b). The $Na_{96}X$ cations were positioned as defined by Vitale et al. (1997). For $Li_{96}X$ and $K_{96}X$ frameworks, the cation distribution was defined by Plévert et al. (1997) and Zhu and Seff (2000), respectively. Divalent cations had the distribution of cations based on $Ca_{48}X$ (Vitale et al. 1995); this same distribution was used for $Mn_{48}X$, $Sr_{48}X$ and $Ba_{48}X$.

Despite the mixing rule proposed by Maurin to calculate the LJ parameters of the extra-framework cation based on Na epsilon and sigma parameters, ionic radius and polarizability, in this test, we used the values proposed by the UFF force field without any changes (Table 6).

Table 5 Percentages of full UFF LJ parameters (ε) for Si and Al atoms

Gas	Framework	ε Si e Al (% UFF)
CO_2	NaX, NaY, USY	22.5
H_2S	NaX, NaY	35
O_2	NaX	22.5
N_2	NaX	56
CH_4	NaX	54

Table 6 Cation LJ parameters based in the UFF force field and the charges used

Cation	σ (Å)	ε (kcal/mol)	Charge (e^{-})
Li^{+}	2.184 (1.673)	0.25 (0.215)	+0.768 and +0.61 (site III)
K^{+}	3.396 (3.483)	0.035 (0.027)	+0.768 and +0.61(site III)
Mn^{2+}	2.638 (2.039)	0.013 (0.316)	+1.536
Ca^{2+}	3.028 (2.612)	0.238 (0.103)	+1.536
Sr^{2+}	3.244 (3.024)	0.235 (0.077)	+1.536
Ba^{2+}	3.299 (3.414)	0.364 (0.084)	+1.536

(*) Maurin et al. (2005b) data in brackets

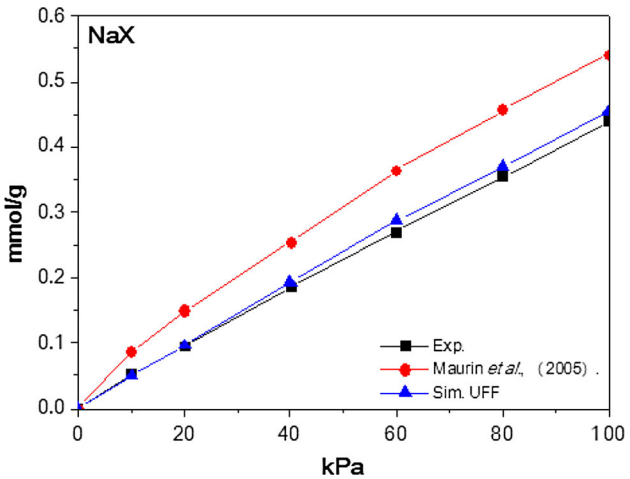

Fig. 8 Experimental (Maurin et al. 2005b) and simulated isotherms (Maurin et al. 2005b and this study: Sim UFF) for N_2 on $Na_{96}X$ at 300 K

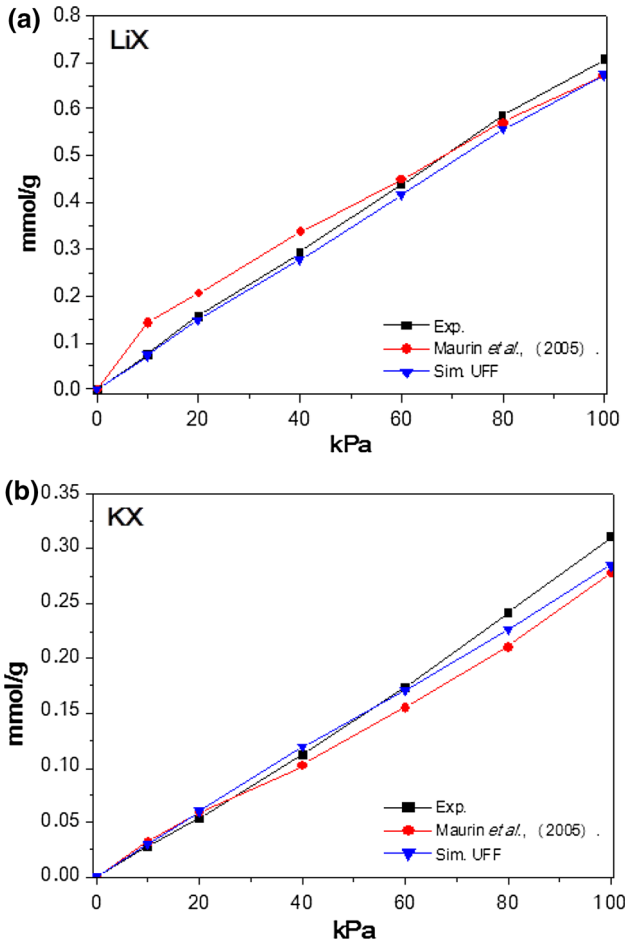

Fig. 9 Experimental (Maurin et al. 2005b) and simulated isotherms (Maurin et al. 2005b and this study: Sim UFF) for N_2 on $Li_{96}X$ (**a**) and $K_{96}X$ (**b**) at 300 K

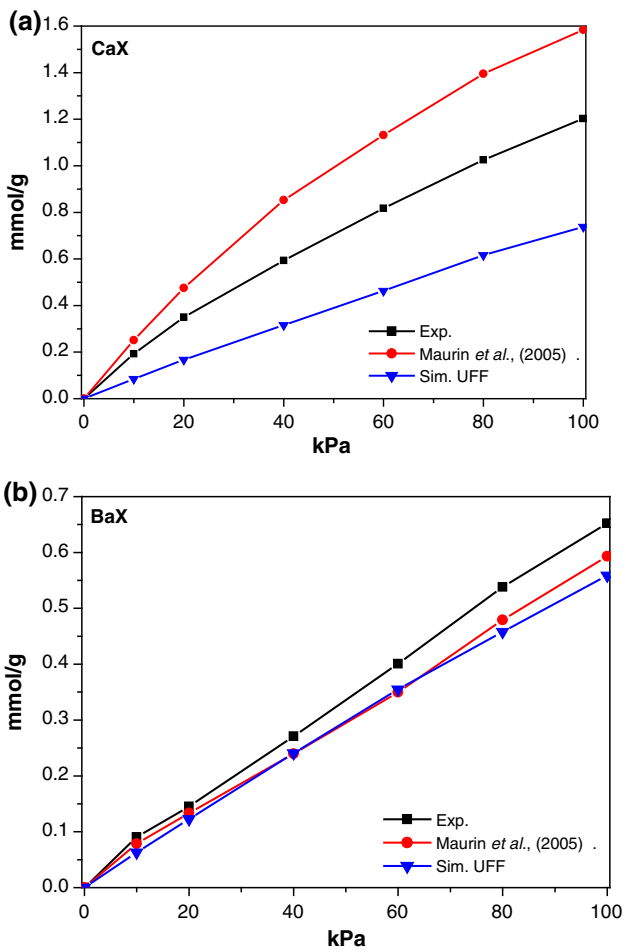

Fig. 10 Experimental (Maurin et al. 2005b) and simulated isotherms (Maurin et al. 2005b and this study: Sim UFF) for N_2 on $Ca_{48}X$ (**a**) and $Ba_{48}X$ (**b**) at 300 K

Figure 8 shows the simulated values for N_2 on $Na_{96}X$ using our force field. For comparison, also shown are the experimental and simulated values obtained by Maurin at the temperature of 300 K. As already discussed in Sect. 3.1.2 the agreement between the simulated and experimental isotherms of N_2 with our force field was very good. The results of Maurin closely follow the trend of the experimental isotherm. After sodium, the test proceeded to the other cations.

The agreement between the experimental isotherms and the simulated isotherms using our force field for monovalent cations was similar to that reported by Maurin (Figs. 9). The transferability among the monovalent series was high, with the adsorption affinity trend LiX > NaX > KX reproduced.

Individual agreements for divalent cations were poor, as occurred in the Maurin study (Figs. 10, 11). Nevertheless, the adsorption affinity trend MnX > CaX > SrX > BaX was also reproduced. The best result of our force field was for BaX (similar to the study of Maurin). An interesting result of our force field was that the experimental trend of close adsorption affinities for CaX and SrX was reproduced. We believe that the poor agreement for divalent cations is related to the value of charge assigned to the cation. Different cations will interact with N_2 at different intensities, and consequently, different amounts of electrons will be transferred.

4 Conclusions

A re-parametrization strategy of a classical force field proved to be effective for predicting the low pressure adsorption equilibrium of CO_2, H_2S, O_2, N_2 and CH_4 on Na-FAU. Experimental CO_2 isotherms in NaX and NaY, exhibiting a crossover pressure, were used in the re-parameterization process. Furthermore, the force field was evaluated for the ability to predict adsorption affinities with monovalent and divalent framework cations. The force

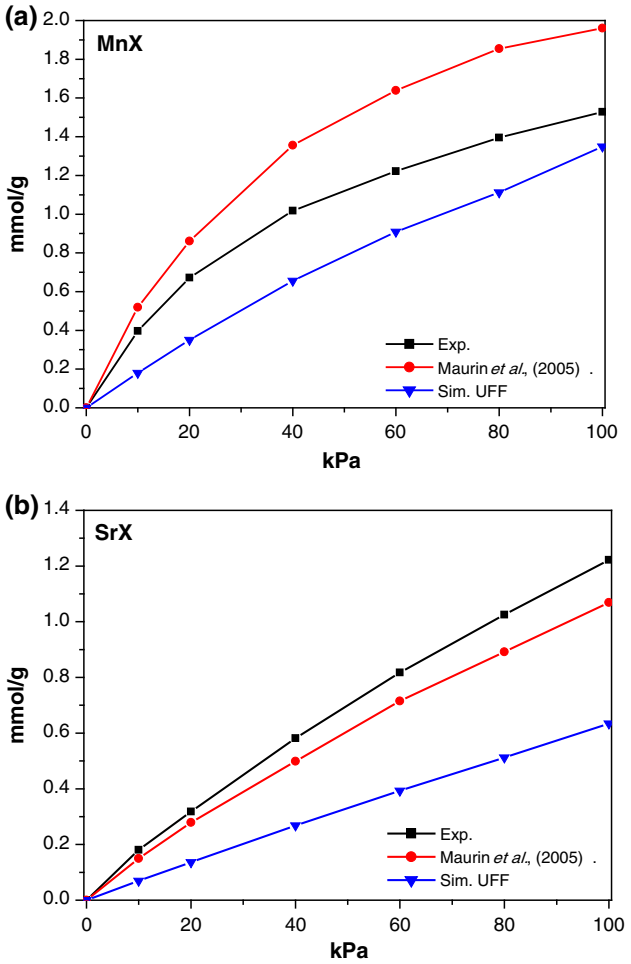

Fig. 11 Experimental (Maurin et al. 2005b) and simulated isotherms (Maurin et al. 2005b and this study: Sim UFF) for N_2 on $Mn_{48}X$ (**a**) and $Sr_{48}X$ (**b**) at 300 K

field presented high transferability within the same gas (N_2) when tested for different monovalent cations (Li, K) and qualitative agreement for the divalent cations (Ca, Mn, Sr, Ba). This modeling strategy can be used to provide initial insight and rapid screening of FAU sieves in mixtures within CO_2 related industrial gases.

Acknowledgments This work is supported by the Brazilian research agencies, CNPq and CAPES.

References

Akten, E.D., Siriwardane, R., Sholl, D.S.: Monte Carlo simulation of single- and binary-component adsorption of CO_2, N_2, and H_2 in zeolite Na-4A. Energy Fuels **17**, 977–983 (2003). doi:10.1021/ef0300038

Bae, T., Hudson, M.R., Mason, J.A., Queen, W.L., Dutton, J.J., Sumida, K., Micklash, K.J., Kaye, S.S., Brown, C.M., Long, J.R.: Energy Environ. Sci. **6**, 128–138 (2013)

Bezus, A.G., Kiselev, A.V., Lopatkin, A.A., Du, P.Q.: Molecular statistical calculation of the thermodynamic adsorption characteristics of zeolites using the atom-atom approximation Part 1.-adsorption of methane by zeolite NaX J. Chem. Soc. Faraday Trans. 2 **74**, 367–379 (1978)

Calero, S., Dubbeldam, D., Krishna, R., Smit, B., Vlugt, T.J.H., Denayer, J.F.M., Martens, J.A., Maesen, T.L.M.: Understanding the role of sodium during adsorption: a force field for alkanes in sodium-exchanged faujasites. J. Am. Chem. Soc. **126**, 11377–11386 (2004)

Cavenati, S., Grande, C.A., Rodrigues, A.E.: Adsorption equilibrium of methane, carbon dioxide, and nitrogen on zeolite 13X at high pressures. J. Chem. Eng. Data **49**, 1095–1101 (2004)

Cejka, J., van Bekkum, H., Corma, A., Schueth, F.: Introduction to Zeolite Science and Practice. Studies in Surface Science and Catalysis, vol. 168, 3rd edn. Elsevier Science, Oxford (2007)

Cruz, A.J., Pires, J., Carvalho, A.P., de Carvalho, M.B.: Physical adsorption of H_2S related to the conservation of works of art: the role of the pore structure at low relative pressure. Adsorption **11**, 569–576 (2005)

Davies, G.M., Seaton, N.A.: The effect of the choice of pore model on the characterization of the internal structure of microporous carbons using pore size distribution. Carbon **36**, 1473–1490 (1998)

Di Lella, A., Desbiens, N., Boutin, A., Demachy, I., Ungerer, P., Bellat, J.-P., Fuchs, A.H.: Molecular simulation studies of water physisorption in zeolites. Phys. Chem. Chem. Phys. **8**, 5396–5406 (2006). doi:10.1039/b610621h

Dubbeldam, D., Calero, S., Vlugt, T.J.H., Krishna, R., Maesen, T.L.M., Beerdsen, E., Smit, B.: Force field parametrization through fitting on inflection points in isotherms. Phys. Rev. Lett. **93**, 088302 (2004)

Fang, H., Kamakoti, P., Ravikovitch, P.I., Aronson, M., Paur, C., Sholl, D.S.: First principles derived, transferable force fields for CO_2 adsorption in Na-exchanged cationic zeolites. Phys. Chem. Chem. Phys. **15**, 12882–12894 (2013)

First, E.L., Faruque Hasan, M.M., Christodoulos, A.: Floudas—discovery of novel zeolites for natural gas purification through combined material screening and process optimization. AIChE J. **60**, 1767–1785 (2014)

Fitch, A.N., Jobic, H., Renouprez, A.: Localization of benzene in sodium-Y-zeolite by powder neutron diffraction. J. Phys. Chem. **90**, 1311–1318 (1986)

Frenkel, D., Smit, B.: Understanding molecular simulation. Academic Press, New York (2002)

García-Sánchez, A., Ania, C.O., Parra, J.B., Dubbeldam, D., Vlugt, T.J.H., Krishna, R., Calero, S.: Transferable force field for carbon dioxide adsorption in zeolites. J. Phys. Chem. C **113**, 8814–8820 (2009). doi:10.1021/jp810871f

Gusev, V.Y., O'Brien, J.A., Seaton, N.A.: A self-consistent method for characterization of activated carbons using supercritical adsorption and grand canonical Monte Carlo simulations. Langmuir **13**, 2815–2821 (1997)

Harris, J.G., Yung, K.H.: Carbon dioxide's liquid-vapor coexistence curve and critical properties as predicted by a simple molecular model. J. Phys. Chem. **99**, 12021–12024 (1995)

Hyun, S.H., Danner, R.P.: Equilibrium adsorption of ethane, ethylene, isobutane, carbon dioxide and their binary mixtures. J. Chem. Eng. Data **27**, 196–200 (1982)

Jayaraman, A., Yang, R.T., Cho, S.-H., Bhat, T.S.G., Choudary, V.N.: Adsorption of nitrogen, oxygen and argon on Na-CeX zeolites. Adsorption **8**, 271–278 (2002)

Jaramillo, E., Chandross, M.: Adsorption of small molecules in LTA zeolites. 1. NH_3, CO_2, and H_2O in zeolite 4A. J. Phys. Chem. B **108**, 20155–20159 (2004)

Kaneco, K., Craknell, R.F., Nicholson, D.: Nitrogen adsorption in slit pores at ambient temperatures: comparison of simulation and experiment. Langmuir **10**, 4606–4609 (1994)

Karge, H.G., Raskó, J.: Hydrogen sulfide adsorption on faujasite-type zeolites with systematically varied Si-Al ratios. Colloid Interface Sci. **64**, 522–532 (1978)

Kim, J.N., Chue, K.T., Kim, K.I., Cho, S.H., Kim, J.D.: Nonisothermal adsorption of nitrogen-carbon dioxide mixture in a fixed-bed of zeolite-X. J. Chem. Eng. Jpn. **27**, 45–51 (1994)

Kiselev, A.V., Du, P.Q.: Molecular statistical calculation of the thermodynamic adsorption characteristics of zeolites using the atom- atom approximation Part 2- adsorption of non-polar and polar inorganic molecules by zeolites of types X and Y. J. Chem. Soc. Faraday Trans. **277**, 1–15 (1981)

Kitagawa, T., Tsunekawa, T., Iwayama, K.: Monte Carlo simulations on adsorptions of benzene and xylenes in sodium-Y zeolites. Microporous Mater. **7**, 227–233 (1996)

Kristof, T., Liszi, J.: Effective intermolecular potential for fluid hydrogen sulfide. J. Phys. Chem. B **101**, 5480–5483 (1997)

Kumar, P., Sung, C.-Y., Muraza, O., Cococcioni, M., Al Hashimi, S., McCormick, A., Tsapatsis, M.: H_2S adsorption by Ag and Cu ion exchanged faujasites. Microporous Mesoporous Mater. **146**, 127–133 (2011). doi:10.1016/j.micromeso.2011.05.014

Llewellyn, P.L., Maurin, G.: Gas adsorption microcalorimetry and modelling to characterize zeolites and related materials. C. R. Chim. **8**, 283–302 (2005)

Liu, D., Wu, Y., Xia, Q., Li, Z., Xi, H.: Experimental and molecular simulation studies of CO2 adsorption on zeolitic imidazolate frameworks: ZIF-8 and amine-modified ZIF-8. Adsorption **19**, 23–37 (2013)

Liu, S., Yang, X.: Gibbs ensemble Monte Carlo simulation of supercritical CO_2 adsorption on NaA and NaX zeolites. J. Chem. Phys. **124**, 244705 (2006)

Lowenstein, W.: The distribution of Al in the tetrahedra of silicates and aluminates. Am. Mineral. **39**, 92–96 (1954)

Lucena, S.M.P., Frutuoso, L.F.A., Silvino, P.F.G., Azevedo, D.C.S., Toso, J.P., Zgrablich, G., Cavalcante, C.L.: Molecular simulation of collection of methane isotherms in carbon material using all-atom and united atom models. Colloids Surf. A **357**, 53–60 (2010)

Maurin, G., Llewellyn, P.L., Bell, R.G.: Adsorption mechanism of carbon dioxide in faujasites: grand canonical monte carlo simulations and microcalorimetry measurements. J. Phys. Chem. B **109**, 16084–16091 (2005a)

Maurin, G., Llewellyn, P.L., Poyet, T., Kuchta, B.: Influence of extra-framework cations on the adsorption properties of X-faujasite systems: microcalorimetry and molecular simulations. J. Phys. Chem. B **109**, 125–129 (2005b)

Simulation, GrandCanonical Monte Carlo, Measurements, Volumetric, Pillai, R.S., Sethia, G., Jasra, V.: Sorption of CO, CH_4, and N_2 in alkali metal ion exchanged zeolite-X. Ind. Eng. Chem. Res. **49**, 5816–5825 (2010)

Plant, D.F., Simperler, A., Bell, R.G.: Adsorption of methanol on zeolites X and Y. An atomistic and quantum chemical study. J. Phys. Chem. B **110**, 6170–6178 (2006)

Plévert, J., Di Renzo, F., Fajula, F.: Structure of dehydrated zeolite Li − LSX by neutron diffraction: evidence for a low-temperature orthorhombic faujasite. J. Phys. Chem. B **101**, 10340–10346 (1997)

Rappé, A.K., Goddard III, W.A.: Charge equilibration for molecular dynamics simulations. J. Phys. Chem. **95**, 3358–3363 (1991)

Rappé, A.K., Casewit, C.J., Cowell, K.S., Goddard III, W.A., Skiff, W.M.: UFF, a full periodic table force field for molecular mechanics and molecular dynamics simulations. J. Am. Chem. Soc. **114**, 10024–10035 (1992)

Silva, J.A.C., Schumann, K., Rodrigues, A.E.: Sorption and kinetics of CO_2 and CH_4 in binderless beads of 13X zeolite. Microporous Mesoporous Mater. **158**, 219–228 (2012)

Skarmoutsos, I., Kampanakis, L.I., Samios, J.: Investigation of the vapor–liquid equilibrium and supercritical phase of pure methane via computer simulations. J. Mol. Liq. **117**, 33–41 (2005)

Su, F., Lu, C.: CO_2 capture from gas stream by zeolite 13X using a dual-column temperature/vacuum swing adsorption. Energy Environ. Sci. **5**, 9021–9027 (2012)

Sun, W., Lin, L.-C., Peng, X., Smit, B.: Computational screening of porous metal-organic frameworks and zeolites for the removal of SO_2 and NOx from flue gases. AIChE J. **60**, 2314–2323 (2014)

Sung, C.-Y., Broadbelt, Linda J., Randall, Q.: Snurr QM/MM study of the effect of local environment on dissociative adsorption in BaY zeolites. J. Phys. Chem. C **113**, 15643–15651 (2009)

Sung, C.-Y., Hashimi, S.Al, McCormick, A., Tsapatsis, M., Cococcioni, M.: Density functional theory study on the adsorption of H_2S and other claus process tail gas components on copper- and silver-exchanged Y zeolites. J. Phys. Chem. C **116**, 3561–3575 (2012)

Tagliabue, M., Bellussi, G., Broccia, P., Carati, A., Millini, R., Pollesel, P., Rizzo, C.: Chem. Eng. J. **210**, 398–403 (2012)

Takahashi, A., Yang, F.H., Yang, R.T., in: M.D. LeVan (Ed.), FOA7—Fundamentals of Adsorption 7, 578–585 (1996)

Thang, H.V., Grajciar, L., Nachtigall, P., Bludsky, O., Areán, C.O., Frydová, E., Bulánek, R.: Adsorption of CO_2 in FAU zeolites: effect of zeolite composition. Catal. Today **227**, 50–56 (2014)

Uytterhoeven, L., Dompas, D., Mortier, W.J.: J. Chem. Soc. Faraday Trans. **88**, 2753–2760 (1992)

Vitale, G., Bull, L.M., Morris, R.E., Cheetham, A.K., Toby, B.H., Coe, C.G., Macdougall, J.E.: Combined neutron and X-ray powder diffraction study of zeolite Ca LSX and a 2H NMR study of its complex with benzene. J. Phys. Chem. B **99**, 16087–16092 (1995)

Vitale, G., Mellot, C.F., Bull, L.M., Cheetham, A.K.: Neutron diffraction and computational study of zeolite NaX: influence of SIII' cations on its complex with benzene. J. Phys. Chem. B **101**, 4559 (1997)

Walton, K.S., Abney, M.B., Levan, M.D.: CO_2 adsorption in Y and X zeolites modified by alkali metal cation exchange. Microporous Mesoporous Mater. **91**, 78–84 (2006)

Watanabe, K., Austin, N., Stapleton, M.R.: Investigation of the air separation properties of zeolites types A, X and Y by Monte Carlo simulations. Mol. Simul. **15**, 197–221 (1995)

Wilmer, C.E., Farha, O.K., Bae, Y.-S., Hupp, J.T., Randall, Q.: Snurr—structure–property relationships of porous materials for carbon dioxide separation and capture. Energy Environ. Sci. **5**, 9849–9856 (2012)

Wong-Ng, W., Kaduk, J.A., Huang, Q., Espinal, L., Li, L., Burress, J.W.: Investigation of NaY zeolite with adsorbed CO_2 by neutron powder diffraction. Microporous Mesopororous Mater. **172**, 95–104 (2013)

Zhu, L., Seff, K.: Reinvestigation of the crystal structure of dehydrated sodium zeolite X. J. Phys. Chem. B **103**, 9512–9518 (1999)

Zhu, L., Seff, K.: Cation crowding in zeolites. Reinvestigation of the crystal structure of dehydrated potassium-exchanged zeolite X. J. Phys. Chem. B **104**, 8946–8951 (2000)